Inorganic Chemistry
Article

Inorg. Chem. **2009**, *48*, 6271–6279 **6271**
DOI: 10.1021/ic900551f

Preparation, Structure, and Metallophilic Interactions of Dinuclear Silver(I) and Copper(I) Complexes of Selenium Diimides

Maarit Risto,[†] Teemu T. Takaluoma,[†] Tom Bajorek,[†] Raija Oilunkaniemi,[†] Risto S. Laitinen,*[,†] and Tristram Chivers*[,‡]

[†]*Department of Chemistry, P.O. Box 3000, FI-90014 University of Oulu, Finland, and*
[‡]*Department of Chemistry, University of Calgary, 2500 University Drive N.W., Calgary, Alberta T2N 1N4, Canada*

Received March 23, 2009

The complexes $[M_2\{\mu\text{-}N,N'\text{-}Se(NR)_2\}_2](CF_3SO_3)_2$ (**1**, M = Ag, R = ^{t}Bu; **2**, M = Ag, R = Ad; **3**, M = Cu, R = ^{t}Bu; **4**, M = Cu, R = Ad; Ad = 1-adamantyl) were prepared in good yields from the reaction of the corresponding selenium diimide with silver or copper triflate in toluene and were characterized in solution using multinuclear NMR spectroscopy. Recrystallization of **1**−**4** from a variety of solvents produced **1**·2CH_2Cl_2, **2**$(AdNH_3)(CF_3SO_3)$ (a few crystals), **3**·2thf, and **4**·1/2C_7H_8, which were characterized by X-ray crystallography. All of these salts contain a metallacyclic $[M_2\{\mu\text{-}N,N'\text{-}Se(NR)_2\}_2]^{2+}$ [M = Ag, Cu; R = ^{t}Bu, Ad] cation, the frameworks of which exhibit M···M close contacts of 2.7384(9), 2.751(2), 2.556(2)−2.569(2), and 2.531(1) Å, respectively. The M···M interaction was further explored by PBE/def-TZVP calculations of the dications $[M_2\{\mu\text{-}N,N'\text{-}Se(NR)_2\}_2]^{2+}$ (M = Ag, Cu; R = H, Me, ^{t}Bu, Ad). The geometry optimizations yielded metric parameters that were in good agreement with experimental values, where available. For both metals, it was observed that the M···M distance became shorter, as the organic substituent on nitrogen became bulkier. At the same time, the metallacyclic framework deviated more significantly from planarity. A survey of related dinuclear silver(I) and copper(I) complexes showed that, while there is some correlation between the bite size and the M···M distance, the latter is more dependent on the deviation from planarity of the $D_2M\cdots MD_2$ fragment. Atoms in molecules calculations clearly showed the presence of a bond critical point between the two silver or copper centers, as well as two ring critical points. Our computational results are consistent with other recent molecular orbital studies at different levels of theory and indicate the existence of d^{10}−d^{10} closed-shell metallophilic interactions in **1**−**4**.

Introduction

Stable monomeric sulfur diimides (RN═S═NR) show a rich coordination chemistry due to the availability of three potential donor sites and two formal π bonds.[1] The bonding mode (see Scheme 1) is dependent on the nature of the metal center as well as on the steric or electronic properties of the diimide ligand. For example, the $M(CO)_5$ unit in the $\sigma(N)$-trigonal complex $[W(CO)_5\{S(NMe)_2\}]$ undergoes a 1,3 shift between the two nitrogen donors,[2] whereas the *tert*-butyl derivative forms a *N*,*N*′-chelated complex $[W(CO)_4\{S(N^tBu)_2\}]$,[3] as has also been observed for some other transition metal complexes (see, for instance, $[Mn_2(CO)_8\{S(N^tBu)_2\}]$[4]) and for compounds with main-group metal halides, for example, $[SnCl_4\{E(N^tBu)_2\}]$ (E = S, Se).[5]

The coordination chemistry of selenium and tellurium diimides has seen much slower progress. In addition to the $SnCl_4$ adduct of $Se(N^tBu)_2$,[5b] dialkyl selenium diimides (RN═Se═NR) have been reported to produce a four-membered SnNSeN ring system with bis(amino)stannylenes.[6] The serendipitous preparation and structural characterization of a palladium complex of a heterocyclic selenium monoimide has recently been described.[7] The dimeric tellurium diimide $(^t$Bu)NTe(μ-N^tBu)$_2$TeN(^{t}Bu) also coordinates

*To whom correspondence should be addressed. Tel.: (3588) 553-1611, (403) 220-5741. Fax: (3588) 553-1608, (403) 289-9488. E-mail: risto.laitinen@oulu.fi, chivers@ucalgary.ca.

(1) (a) Chivers, T. *A Guide to Chalcogen-Nitrogen Chemistry*; World Scientific Publishing Co. Pte. Ltd.: Singapore, 2005. (b) Chivers, T.; Laitinen, R. S. *Chalcogen-Nitrogen Chemistry. Handbook of Chalcogen Chemistry, New Perspectives in Sulfur, Selenium and Tellurium*; RSC Press: Cambridge, U. K., 2007; pp 223−285.

(2) (a) Meij, R.; Kuyper, J.; Stufkens, D. J.; Vrieze, K. *J. Organomet. Chem.* **1976**, *110*, 219. (b) Meij, R.; Kaandorp, T. A. M.; Stufkens, D. J.; Vrieze, K. *J. Organomet. Chem.* **1977**, *128*, 203.

(3) Meij, R.; Olie, K. *Cryst. Struct. Commun.* **1975**, *4*, 515.

(4) Mahabiersing, C.; de Lange, W. G. J.; Goubitz, K.; Stufkens, D. J. *J. Organomet. Chem.* **1993**, *461*, 127.

(5) (a) Roesky, H. W.; Schmidt, H.-G.; Noltemeyer, M.; Sheldrick, G. M. *Chem. Ber.* **1983**, *116*, 1411. (b) Gindl, J.; Björgvinsson, M.; Roesky, H. W.; Freire-Erdbrügger, C.; Sheldrick, G. M. *J. Chem. Soc., Dalton Trans.* **1993**, 811.

(6) Wrackmeyer, B.; Köhler, C.; Milius, W.; Herberhold, M. *Z. Anorg. Allg. Chem.* **1995**, *621*, 1625.

(7) Lozan, V.; Kerstin, B. *Dalton Trans.* **2007**, 4511.

Published on Web 06/05/2009

Scheme 1. Bonding Modes in Complexes of Sulfur Diimides

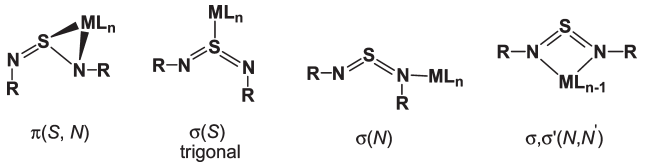

Scheme 2. $[Ag_2\{\mu\text{-}N,N'\text{-}Te_2(N^tBu)_4\}_2]^{2+}$ Dication

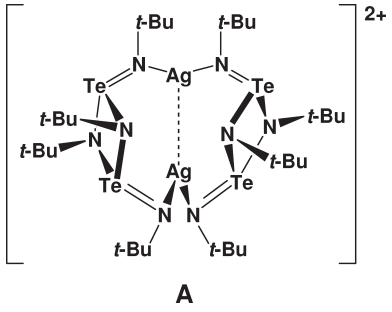

to metal centers via exocyclic nitrogen donors and can act as a chelating or bridging ligand, as exemplified by complex formation with $HgCl_2$[8] or $Ag(CF_3SO_3)$ and $Cu(CF_3SO_3)$.[9]

Interestingly, $[Ag_2\{\mu\text{-}N,N'\text{-}Te_2(N^tBu)_4\}_2](CF_3SO_3)_2$, which contains a macrocyclic dinuclear cation **A** (see Scheme 2), shows a Ag···Ag close contact of 2.888(2) Å that can be attributed to d^{10}–d^{10} closed-shell interaction.[9] Such a metallophilic interaction is well-established for a variety of gold complexes[10] but is rather controversial for Ag(I) and Cu(I).[11]

The present contribution discusses the formation and stereochemistry of coinage metal complexes of selenium diimides, specifically the preparation and structural characterization of Ag^+ and Cu^+ complexes of *tert*-butyl (^{t}Bu) and adamantyl (Ad) selenium diimides. The single-crystal X-ray structures **1**·$2CH_2Cl_2$, **2**$(AdNH_3)(CF_3SO_3)$, **3**·2thf, and **4**·$1/2C_7H_8$ are described. In addition to the ligand properties of selenium diimides, we were interested in assessing the magnitude of d^{10}–d^{10} interactions through the consideration of structural trends and DFT calculations.

Experimental Section

General. All reactions and manipulations of air- and moisture-sensitive products were carried out under an inert atmosphere by using a standard drybox or Schlenk techniques. $SeCl_4$ (Aldrich), 1-adamantylamine ($AdNH_2$, Aldrich), $Ag(CF_3SO_3)$ (Alfa Aesar), and $Cu(CF_3SO_3)\cdot 1/2C_6H_6$ (Alfa Aesar) were used as purchased. $^tBuNH_2$ (Aldrich) was distilled over KOH and stored over molecular sieves. $Se(N^tBu)_2$ and $Se(NAd)_2$ were prepared from $SeCl_4$ and the primary amines $^tBuNH_2$[13] and $AdNH_2$,[14] respectively. Toluene and tetrahydrofuran were dried by distillation over Na/benzophenone, and CH_2Cl_2 was dried over P_4O_{10} under an argon atmosphere prior to use.

NMR Spectroscopy. The ^{1}H NMR spectra were recorded in CD_2Cl_2 on a Bruker DPX 200 spectrometer operating at 200.13 MHz. The spectral width was 4.4 kHz. The pulse width was 6.6 μs, and the pulse delay was 1.0 s. The ^{14}N and ^{77}Se NMR spectra were recorded in CH_2Cl_2 on a Bruker DPX400 spectrometer operating at 28.91 and 76.41 MHz, respectively. The ^{14}N and ^{77}Se NMR spectra were recorded unlocked. The typical respective spectral widths were 20.00 and 90.00 kHz, and the pulse widths were 12.0 and 6.7 μs. The pulse delay for nitrogen and selenium was 10.0 ms and 2.0 s, respectively. The ^{1}H NMR spectra were referenced to the solvent resonance and are reported relatively to Me_4Si. The ^{14}N NMR spectra are reported relatively to neat CH_3NO_2. All ^{77}Se NMR spectra were referenced externally to a saturated aqueous solution of selenium dioxide, and the chemical shifts are reported relatively to neat Me_2Se [$\delta(Me_2Se) = \delta(SeO_2) + 1302.6$].[15]

Preparation of $[Ag_2\{\mu\text{-}N,N'\text{-}Se(N^tBu)_2\}_2](CF_3SO_3)_2$ (1). A solution of $Se(N^tBu)_2$ (0.316 g, 1.43 mmol) in 10 mL of toluene was added dropwise to a stirred slurry of $Ag(CF_3SO_3)$ (0.368 g, 1.43 mmol) in 10 mL of toluene. After 15 min at −80 °C, the reaction mixture was warmed slowly to room temperature and stirred for 3 h. The solution was decanted, and the yellow solid **1** was dried under vacuum conditions. Yield: 0.411 g (60%). Anal. calcd for $C_9H_{18}AgF_3N_2O_3SSe$: C, 22.61; H, 3.79; N, 5.86; S, 6.71%. Found: C, 22.25; H, 4.15; N, 5.45; S, 6.68%. NMR: δ ^{1}H (CD_2Cl_2, 298 K) 1.62 ppm; δ ^{14}N (CH_2Cl_2, 298 K) 0 ppm; δ ^{77}Se (CH_2Cl_2, 298 K) 1798 ppm. X-ray-quality crystals of **1**·$2CH_2Cl_2$ were obtained by recrystallization from CH_2Cl_2 at −20 °C.

Preparation of $[Ag_2\{\mu\text{-}N,N'\text{-}Se(NAd)_2\}_2](CF_3SO_3)_2$ (2). A solution of $Se(NAd)_2$ (0.201 g, 0.53 mmol) in 10 mL of toluene was added dropwise to a stirred slurry of $Ag(CF_3SO_3)$ (0.137 g, 0.53 mmol) in 10 mL of toluene. After 20 min at −80 °C, the reaction mixture was warmed slowly to room temperature and stirred further for 1.5 h. The solvent was removed under vacuum conditions to give **2** as a yellow solid. Yield: 0.278 g (82%). Anal. calcd for $C_{21}H_{30}AgF_3N_2O_3SSe$: C, 39.76; H, 4.73; N, 4.42; S, 5.06%. Found: C, 38.94; H, 5.01; N, 3.84; S, 4.91%. NMR (CH_2Cl_2, 298 K): δ ^{77}Se 1781 ppm. Crystallization from the reaction solution at −20 °C afforded a small amount of X-ray-quality crystals of **2**$(AdNH_3)(CF_3SO_3)$.

Preparation of $[Cu_2\{\mu\text{-}N,N'\text{-}Se(N^tBu)_2\}_2](CF_3SO_3)_2$ (3). A solution of $Se(N^tBu)_2$ (0.172 g, 0.78 mmol) in 10 mL of toluene was added dropwise to a stirred slurry of $Cu(CF_3SO_3)\cdot 1/2C_6H_6$ (0.196 g, 0.78 mmol) in 10 mL of toluene. After 30 min at −80 °C, the reaction mixture was warmed slowly to room temperature and stirred further for 1.5 h. The solvent was

(8) Chivers, T.; Schatte, G. *Can. J. Chem.* **2003**, *81*, 1307.
(9) (a) Chivers, T.; Parvez, M.; Schatte, G. *Angew. Chem., Int. Ed.* **1999**, *38*, 2217. (b) Chivers, T.; Parvez, M.; Schatte, G. *Inorg. Chem.* **1999**, *38*, 5171.
(10) (a) Pyykkö, P. *Chem. Rev.* **1997**, *97*, 597. (b) Pyykkö, P. *Angew. Chem., Int. Ed. Engl.* **2004**, *43*, 4412. (c) Pyykkö, P. *Chem. Soc. Rev.* **2008**, *37*, 1967. (d) Van den Ancker, T. R.; Bhargava, S. K.; Mohr, F.; Papadopoulos, S.; Raston, C. L.; Skelton, B. W.; White, A. H. *J. Chem. Soc., Dalton Trans.* **2001**, 3069.
(11) Experimental evidence on close M···M (M = Ag, Cu) contacts is still rather sparse, and there are theoretical arguments both for and against the stabilization of the complexes by ligand-unsupported M···M interactions at different levels of theory. The experimental data and theoretical arguments are reviewed and discussed in refs 9 and 12 (see also references cited therein).
(12) (a) Merz, K. M.; Hoffmann, R. *Inorg. Chem.* **1988**, *27*, 2120. (b) Cotton, F. A.; Feng, X.; Matusz, M.; Poli, R. *J. Am. Chem. Soc.* **1988**, *110*, 7077. (c) Kölmel, C.; Aldrich, R. *J. Phys. Chem.* **1990**, *94*, 5536. (d) Singh, K.; Long, J. R.; Stavropoulos, P. *J. Am. Chem. Soc.* **1997**, *119*, 2942. (e) Fernández, E. J.; Lopez-de-Luzuriaga, J. M.; Monge, M.; Rodriguez, M. A.; Crespo, O.; Gimeno, M. C.; Laguna, A.; Jones, P. G. *Inorg. Chem.* **1998**, *37*, 6002. (f) Wang, Q.-M.; Mak, T. C. *J. Am. Chem. Soc.* **2001**, *123*, 7594. (g) Vehlow, K.; Köhler, K.; Blechert, S.; Dechert, S.; Meyer, F. *Eur. J. Inorg. Chem.* **2005**, 2727. (h) Olson, L. P.; Whitcomb, D. R.; Rajeswaran, M.; Blanton, T. N.; Stwertka, B. J. *Chem. Mater.* **2006**, *18*, 1667. (i) Ray, L.; Shaikh, M. M.; Ghosh, P. *Inorg. Chem.* **2008**, *47*, 230.
(13) Herberhold, M.; Jellen, W. *Z. Naturforsch.* **1986**, *41b*, 144.
(14) Maaninen, T.; Laitinen, R.; Chivers, T. *Chem. Commun.* **2002**, 1812.
(15) Burns, R. C.; Collins, M. J.; Gillespie, R. J.; Schrobilgen, G. J. *Inorg. Chem.* **1986**, *25*, 4465.

Table 1. Details of the Structure Determination of $[Ag_2\{\mu\text{-}N,N'\text{-}Se(N^tBu)_2\}_2](CF_3SO_3)_2\cdot 2CH_2Cl_2$ {**1**·$2CH_2Cl_2$}, $[Ag_2\{\mu\text{-}N,N'\text{-}Se(NAd)_2\}_2](AdNH_3)(CF_3SO_3)_3$ {**2**$(AdNH_3)(CF_3SO_3)$}, $[Cu_2\{\mu\text{-}N,N'\text{-}Se(N^tBu)_2\}_2](CF_3SO_3)_2\cdot$2thf {**3**·2thf}, and $[Cu_2\{\mu\text{-}N,N'\text{-}Se(NAd)_2\}_2](CF_3SO_3)_2\cdot 1/2C_7H_8$ {**4**·$1/2C_7H_8$}

	1·$2CH_2Cl_2$	**2** $(AdNH_3)(CF_3SO_3)$	**3**·2thf	**4**·$1/2C_7H_8$
empirical formula	$C_{20}H_{40}Ag_2Cl_4F_6N_4O_6S_2Se_2$	$C_{64}H_{96}Ag_2F_{12}N_6O_{12}S_4Se_2$	$C_{26}H_{52}Cu_2F_6N_4O_8S_2Se_2$	$C_{45.5}H_{64}Cu_2F_6N_4O_6S_2Se_2$
fw	1126.14	1871.37	1011.84	1226.13
temp (K)	120(2)	120(2)	120(2)	120(2)
cryst syst	monoclinic	triclinic	monoclinic	monoclinic
space group	$C2/c$	$P\bar{1}$	$P2_1/c$	$C2/c$
a (Å)	24.414(5)	11.453(2)	18.929(4)	28.586(6)
b (Å)	11.849(2)	12.007(2)	11.480(2)	14.349(3)
c (Å)	15.950(3)	15.581(3)	19.452(4)	25.934(5)
α (deg)		68.81(3)		
β (deg)	123.71(3)	70.67(3)	108.01(3)	112.75(3)
γ (deg)		74.18(3)		
V (Å^3)	3838.2(18)	1856.5(6)	4020(1)	9810(3)
Z	4	1	4	8
F(000)	2208	952	2048	5000
D_{calcd} (g cm^{-3})	1.949	1.674	1.672	1.660
μ(Mo Kα) (mm^{-1})	3.372	1.712	3.047	2.511
cryst size (mm)	0.30 × 0.10 × 0.10	0.10 × 0.08 × 0.05	0.20 × 0.20 × 0.05	0.15 × 0.12 × 0.12
independent/observed reflns	3680/3331	6250/3234	6717/3572	8502/5337
R_{INT}	0.0699	0.1235	0.1361	0.1311
R_1/wR_2 $[I \geq 2\sigma(I)]^a$	0.0554/0.1542	0.0743/0.1609	0.0593/0.1114	0.0507/0.0938
R_1/wR_2 (all data)^a	0.0601/0.1604	0.1471/0.1882	0.1427/0.1324	0.1053/0.1078
GOF	1.198	1.030	1.002	0.999
max. min. heights in final difference Fourier synthesis (e Å^{-3})	1.651, −1.428	1.671, −0.802	0.997, −0.857	0.870, −0.851

$^aR_1 = \sum||F_o| - |F_c||/\sum|F_o|$, $wR_2 = [\sum w(F_o^2 - F_c^2)^2/\sum wF_o^4]^{1/2}$.

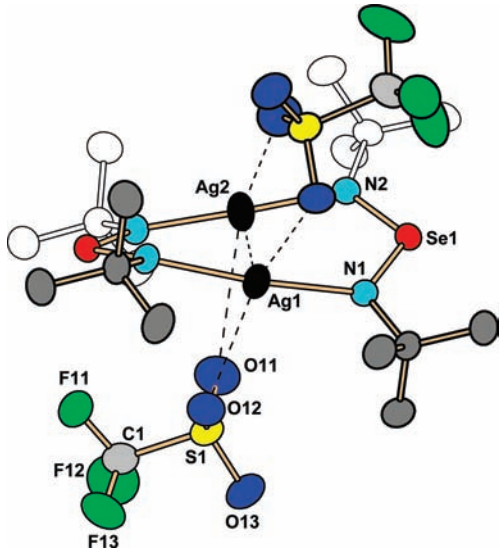

Figure 1. The molecular structure of **1**·$2CH_2Cl_2$ indicating the numbering of atoms. The thermal ellipsoids have been drawn at the 50% probability level. The hydrogen atoms and the solvent molecules have been omitted for clarity.

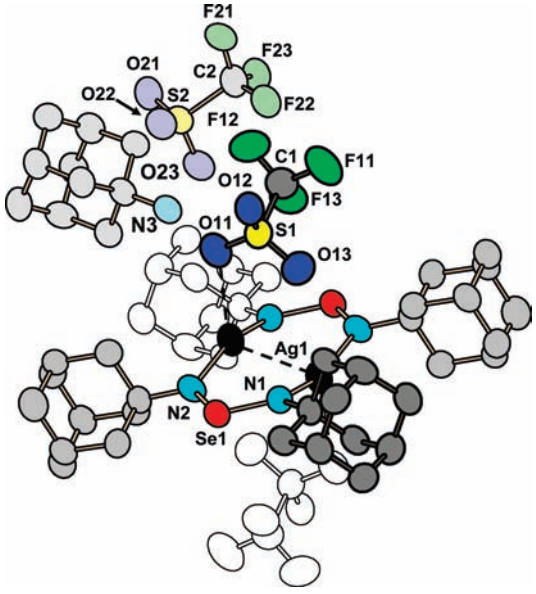

Figure 2. The molecular structure of **2**$(AdNH_3)(CF_3SO_3)$ indicating the numbering of atoms. The thermal ellipsoids have been drawn at the 50% probability level. The hydrogen atoms have been omitted for clarity.

removed under vacuum conditions to give **3** as a dark brown solid. Yield: 0.241 g (71%). Anal. calcd for $C_9H_{18}CuF_3N_2O_3SSe$: C, 24.92; H, 4.18; N, 6.46; S, 7.39%. Found: C, 23.69; H, 3.99; N, 5.68; S, 8.36%. NMR: δ ^{1}H (CD_2Cl_2, 298 K) 1.77 ppm; δ ^{14}N (CH_2Cl_2, 298 K) −36 ppm; δ ^{77}Se (CH_2Cl_2, 298 K) 1783 ppm. Recrystallization from CH_2Cl_2-thf (thf = tetrahydrofuran, C_4H_8O) solution at −20 °C afforded X-ray-quality crystals of **3**·2thf.

Preparation of $[Cu_2\{\mu\text{-}N,N'\text{-}Se(NAd)_2\}_2](CF_3SO_3)_2$ (4). A solution of $Se(NAd)_2$ (0.200 g, 0.53 mmol) in 15 mL of toluene was added dropwise to a stirred slurry of $Cu(CF_3SO_3)\cdot 1/2C_6H_6$ (0.135 g, 0.53 mmol) in 10 mL of toluene. After 45 min at −80 °C, the reaction mixture was warmed slowly to room temperature and stirred further for 2 h. The solvent was removed under vacuum conditions to give **4** as a dark brown solid. Yield: 0.282 g (90%). Anal. calcd for $C_{21}H_{30}CuF_3N_2O_3SSe$: C, 42.74; H, 5.12; N, 4.75; S, 6.01%. Found: C, 42.95; H, 5.11; N, 4.26; S, 5.56%. NMR (CH_2Cl_2, 298 K): δ ^{77}Se 1773 ppm. X-ray-quality crystals of **4**·$1/2C_7H_8$ were isolated by crystallization from toluene at −20 °C.

X-Ray Crystallography. Diffraction data of **1**·$2CH_2Cl_2$, **2**$(AdNH_3)(CF_3SO_3)$, **3**·2thf, and **4**·$1/2C_7H_8$ were collected on a Nonius Kappa CCD diffractometer at 120 K using graphite-monochromated Mo Kα radiation (λ = 0.71073 Å; 55 kV, 25 mA). Crystal data and the details of structure determinations are given in Table 1.

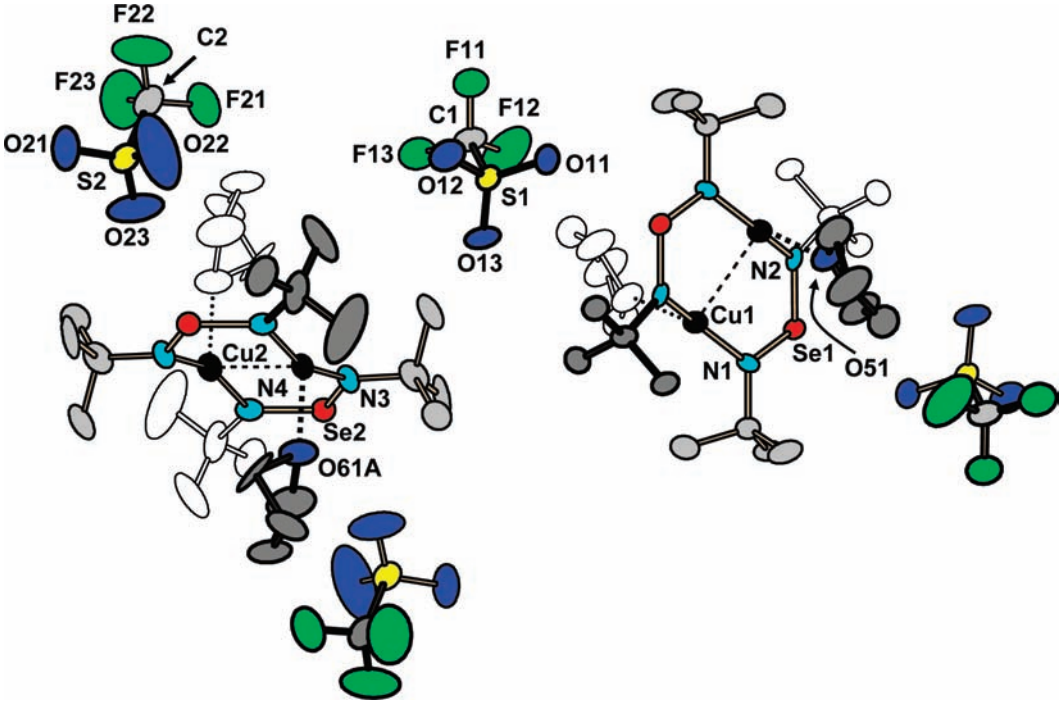

Figure 3. The molecular structure of **3**·2thf indicating the numbering of atoms. The thermal ellipsoids have been drawn at the 50% probability level. The hydrogen atoms and the noncoordinating tetrahydrofuran molecule have been omitted for clarity. One of the *tert*-butyl groups is disordered and assumes two orientations in the lattice. Only the more abundant orientation of the pair is shown in the figure.

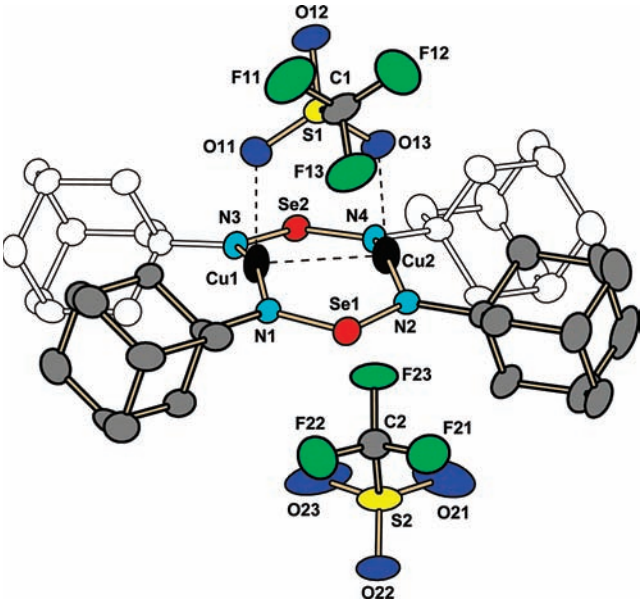

Figure 4. The molecular structure of **4**·1/2C_7H_8 indicating the numbering of atoms. The thermal ellipsoids have been drawn at the 50% probability level. The hydrogen atoms and the solvent molecule have been omitted for clarity.

Structures were solved by direct methods using SIR-92[16] and refined using SHELXL-97.[17] After the full-matrix least-squares refinement of the non-hydrogen atoms with anisotropic thermal parameters, the hydrogen atoms were placed in calculated positions in the CH_3 groups (C−H = 0.98 Å), in the CH_2 groups (C−H = 0.99 Å), in the CH groups (C−H = 1.00 Å), and in NH_3 groups (N−H = 0.91 Å). In the final refinement, the hydrogen atoms were riding with the carbon and nitrogen atoms to which they were bonded. The isotropic thermal parameters of the hydrogen atoms were fixed at 1.2 (CH_2, CH) and 1.5 (CH_3, NH_3) times that of the corresponding carbon and nitrogen atoms, respectively. The scattering factors for the neutral atoms were those incorporated with the program.

One *tert*-butyl group and the coordinated thf molecule in **3**·2thf and the solvent toluene molecule in **4**·1/2C_7H_8 were found to be disordered. In **3**·2thf, the disorder was resolved by constraining during the refinement the sums of the site occupancy factors of the two disordered pairs to unity and keeping the anisotropic thermal parameters of the equivalent atoms of the disordered pair equal. The disordered solvent molecule occupied two symmetry-equivalent orientations with a fixed site-occupancy factor of 0.5.

Computational Details. The geometry optimizations of the model cations $[M_2\{\mu\text{-}N,N'\text{-}Se(NR)_2\}_2]^{2+}$ (M = Cu, Ag; R = H, Me, ^{t}Bu, Ad) were performed with a Turbomole 5.10 program package[18] at a pure DFT level of theory employing the PBE functional[19] and def-TZVP basis sets.[20] The nature of the optimized stationary points was confirmed by calculating the fundamental vibrations. The properties of bond critical points for the optimized geometries were calculated with the program AIM2000[21] using wave functions obtained by the use of the

(16) Altomare, A.; Cascarano, G.; Giacovazzo, C.; Gualardi, A. *J. Appl. Crystallogr.* **1993**, *26*, 343.
(17) Sheldrick, G. M. *Acta Crystallogr.* **2008**, *64A*, 112.

(18) Ahlrichs, R.; Bär, M.; Häser, M.; Horn, H.; Kölmel, C. *Chem. Phys. Lett.* **1989**, *162*, 165. (b) TURBOMOLE V5.10 2008, a development of University of Karlsruhe and Forschungszentrum Karlsruhe GmbH, 1989−2007, TURBOMOLE GmbH, since 2007; available from http://www.turbomole.com (accessed May 2009).
(19) (a) Dirac, P. A. M. *Proc. R. Soc. London A* **1929**, *123*, 714. (b) Slater, J. C. *Phys. Rev.* **1951**, *81*, 385. (c) Perdew, J. P.; Wang, Y. *Phys. Rev. B* **1992**, *45*, 13244. (d) Perdew, J. P.; Burke, K.; Ernzerhof, M. *Phys. Rev. Lett.* **1996**, *77*, 3865.
(20) (a) Eichkorn, K.; Weigend, F.; Treutler, O.; Ahlrichs, R. *Theor. Chem. Acc.* **1997**, *97*, 119. (b) Weigend, F.; Ahlrichs, R. *Phys. Chem. Chem. Phys.* **2005**, *7*, 3297. (c) Andrae, D.; Haeussermann, U.; Dolg, M.; Stoll, H.; Preuss, H. *Theor. Chim. Acta* **1990**, *77*, 123.
(21) Biegler-König, F.; Schönbohm, J. *J. Comput. Chem.* **2002**, *23*, 1489.

Table 2. Selected Bond Lengths (Å) and Angles (deg) in the Dications of $[Ag_2\{\mu\text{-}N,N'\text{-}Se(N^tBu)_2\}_2](CF_3SO_3)_2\cdot 2CH_2Cl_2$ {**1**·$2CH_2Cl_2$}, $[Ag_2\{\mu\text{-}N,N'\text{-}Se(NAd)_2\}_2](AdNH_3)(CF_3SO_3)_3$ {**2**$(AdNH_3)(CF_3SO_3)$}, $[Cu_2\{\mu\text{-}N,N'\text{-}Se(N^tBu)_2\}_2](CF_3SO_3)_2\cdot$2thf {**3**·2thf}, and $[Cu_2\{\mu\text{-}N,N'\text{-}Se(NAd)_2\}_2](CF_3SO_3)_2\cdot 1/2C_7H_8$ {**4**·$1/2C_7H_8$}

	1·$2CH_2Cl_2$		**2** $(AdNH_3)(CF_3SO_3)$		**3**·2thf		**4**·$1/2C_7H_8$	
M···M	Ag1···Ag2	2.7384(9)	Ag1···Ag1[d]	2.751(2)	Cu1···Cu1[a]	2.569(2)	Cu1···Cu2	2.531(1)
					Cu2···Cu2[b]	2.556(2)		
M−N	Ag1−N1	2.226(4)	Ag1−N1	2.152(7)	Cu1−N1	1.912(5)	Cu1−N1	1.901(4)
					Cu1−N2[a]	1.913(6)	Cu1−N3	1.907(4)
	Ag2−N2	2.108(4)	Ag1−N2	2.161(7)	Cu2−N3	1.896(6)	Cu2−N2	1.917(4))
					Cu2−N4	1.904(6)	Cu2−N4	1.915(4
Se−N	Se1−N1	1.712(4)	Se1−N1	1.749(7)	Se1−N1	1.714(6)	Se1−N1	1.728(4)
					Se1−N2	1.729(6)	Se1−N2	1.715(4)
	Se1−N2	1.712(4)	Se1−N2	1.719(7)	Se2−N3	1.709(6)	Se2−N3	1.716(4)
					Se2−N4	1.721(7)	Se2−N4	1.708(4)
N−M−N	N1−Ag1−N1[c]	168.6(2)	N1−Ag1−N2[d]	157.7(3)	N1−Cu1−N2[a]	158.8(2)	N1−Cu1−N3	161.4(2)
	N2−Ag2−N2[c]	176.6.(2)			N3−Cu2−N4[b]	157.9(3)	N2−Cu2−N4	160.2(2)
M−N−Se	Se1−N1−Ag1	125.7(2)	Se1−N1−Ag1	126.9(3)	Se1−N1−Cu1	126.1(3)	Cu1−N1−Se1	125.5(2)
					Se1−N2−Cu1[a]	123.0(3)	Cu1−N3−Se2	125.5(2)
	Se1−N2−Ag2	124.7(2)	Se1−N2−Ag1[d]	124.7(4)	Se2−N3−Cu2	124.8(4)	Cu2−N2−Se1	125.9(2)
					Se2−N4−Cu2[b]	125.1(4)	Cu2−N4−Se2	124.7(2)
N−M−N−Se	N1[c]−Ag1−N1-Se1	29.5(2)	N1−Ag1−N2[d]−Se1[d]	102.9(7)	N2[a]−Cu2−N1−Se1	−112.9(7)	N1−Cu1−N3−Se2	−108.2(5)
							N3−Cu1−N1−Se1	108.0(5)
	N2[c]−Ag2−N2-Se1	−158.2(2)	N2[d]−Ag1−N1−Se1	−108.1(7)	N4[b]−Cu2−N3−Se2	−114.3(7)	N2−Cu2−N4−Se2	109.6(5)
							N4−Cu2−N2−Se1	−106.2(5)
N−Se−N−M	N2−Se1−N1−Ag1	−20.9(3)	N2−Se1−N1−Ag1	17.5(5)	N1−Se1−N2−Cu1[a]	−16.1(4)	N1−Se1−N2−Cu2	2.4(3)
					N2−Se1−N1−Cu1	8.3(4)	N2−Se1−N1−Cu1	−2.6(3)
	N1−Se1−N2−Ag2	−6.5(3)	N1−Se1−N2−Ag1[d]	10.0(5)	N3−Se2−N4−Cu2[b]	13.5(5)	N3−Se2−N4−Cu2	−6.4(3)
					N4−Se2−N3−Cu2	12.4(5)	N4−Se2−N3−Cu1	4.8(3)

[a] $-x, -y+1, -z$. [b] $-x+1, -y, -z$. [c] $-x, y, -z+1/2$. [d] $-x+1, -y, -z$.

program Gamess-US.[22a] Gamess-US computations used the TZVP basis as implemented in the Gaussian 03 program package for all atoms, except that the DGDZVP basis set was used for the Ag atoms.[22b]

In order to obtain more reliable information about the M···M interactions, higher-level computations were performed on $[M_2\{\mu\text{-}N,N'\text{-}Se(NH)_2\}_2]^{2+}$ by using, in addition to the PBE functional, also RIMP2 and RICC2 [23] calculations. The computations were performed involving def2-TZVP,[20b,20c] def2-TZVPP,[20c,24a] and def2-QZVPP[24b−24g] basis sets.

(22) (a) Gamess, version 24 MAR 2007 (R1); Iowa State University: Schmidt, M. W.; Baldridge, K. K.; Boatz, J. A.; Elbert, S. T.; Gordon, M. S.; Jensen, J. H.; Koseki, S.; Matsunaga, N.; Nguyen, K. A.; Su, S.; Windus, T. L.; Dupuis, M.; Montgomery, J. A. *J. Comput. Chem.* **1993**, *14*, 1347. (b) Gaussian 03: Frisch, M. J.; Trucks, G. W.; Schlegel, H. B.; Scuseria, G. E.; Robb, M. A.; Cheeseman, J. R.; Montgomery J. A.,; Vreven, T.; Kudin, K. N.; Burant, J. C.; Millam, J. M.; Iyengar, S. S.; Tomasi, J.; Barone, V.; Mennucci, B.; Cossi, M.; Scalmani, G.; Rega, N.; Petersson, G. A.; Nakatsuji, H.; Hada, M.; Ehara, M.; Toyota, K.; Fukuda, R.; Hasegawa, J.; Ishida, M.; Nakajima, T.; Honda, Y.; Kitao, O.; Nakai, H.; Klene, M.; Li, X.; Knox, J. E.; Hratchian, H. P.; Cross, J. B.; Bakken, V.; Adamo, C.; Jaramillo, J.; Gomperts, R.; Stratmann, R. E.; Yazyev, O.; Austin, A. J.; Cammi, R.; Pomelli, C.; Ochterski, J. W.; Ayala, P. Y.; Morokuma, K.; Voth, G. A.; Salvador, P.; Dannenberg, J. J.; Zakrzewski V. G.; Dapprich, S.; Daniels, A. D.; Strain, M. C.; Farkas, O.; Malick, D. K.; Rabuck, A. D.; Raghavachari, K.; Foresman, J. B.; Ortiz, J. V.; Cui, Q.; Baboul, A. G.; Clifford, S.; Cioslowski, J.; Stefanov, B. B.; Liu, G.; Liashenko, A.; Piskorz, P.; Komaromi, I.; Martin, R. L.; Fox, D. J.; Keith, T.; Al-Laham, M. A.; Peng, C. Y.; Nanayakkara, A.; Challacombe, M.; Gill, P. M. W.; Johnson, B.; Chen, W.; Wong, M. W.; Gonzalez, C.; Pople, J. A. *Gaussian 03*, revision D.02; Gaussian, Inc.: Wallingford, CT, 2004.

(23) (a) Weigend, F.; Häser, M. *Theor. Chem. Acc.* **1997**, *97*, 331. (b) Weigend, F.; Häser, M.; Patzelt, H.; Ahlrichs, R. *Chem. Phys. Lett.* **1998**, *294*, 143. (c) Christiansen, O.; Koch, H.; Jørgensen, P. *Chem. Phys. Lett.* **1995**, *243*, 409. (d) Hättig, C.; Weigend, F. *J. Chem. Phys.* **2000**, *113*, 5154. (e) Hättig, C. *J. Chem. Phys.* **2003**, *118*, 7751. (f) Hättig, C.; Hellweg, A.; Köhn, A. *Phys. Chem. Chem. Phys.* **2006**, *8*, 1159.

(24) (a) Weigend, F.; Furche, F.; Ahlrichs, R. *J. Chem. Phys.* **2003**, *119*, 12753. (b) Woon, D. E.; Dunning, T. H.Jr. *J. Chem. Phys.* **1993**, *98*, 1358. (c) Kendall, R. A.; Dunning, T. H.Jr.; Harrison, R. J. *J. Chem. Phys.* **1992**, *96*, 6796. (d) Dunning, T. H.Jr. *J. Chem. Phys.* **1989**, *90*, 1007. (e) Peterson, K. A.; Woon, D. E.; Dunning, T. H.Jr. *J. Chem. Phys.* **1994**, *100*, 7410. (f) Wilson, A.; van Mourik, T.; Dunning, T. H.Jr. *THEOCHEM* **1997**, *388*, 339. (g) Davidson, E. R. *Chem. Phys. Lett.* **1996**, *260*, 514.

Results and Discussion

General. The moisture-sensitive selenium diimide complexes of silver and copper **1**−**4** were obtained in 60−90% yields by the reactions of equimolar amounts of $Se(NR)_2$ (R = ^{t}Bu, Ad) and $M(CF_3SO_3)$ (M = Ag, Cu) in toluene (eq 1). All complexes **1**−**4** are moisture-sensitive, but the yellow silver complexes **1** and **2** are more stable in the air than the dark brown copper complexes **3** and **4**.

$$2M(CF_3SO_3) + 2Se(NR)_2 \rightarrow [M_2\{Se(NR)_2\}_2](CF_3SO_3)_2$$
$$M = Ag, Cu \; R = {}^tBu, Ad \qquad \mathbf{1}{:}M = Ag, R = {}^tBu; \mathbf{2}{:}M = Ag, R = Ad$$
$$\mathbf{3}{:}M = Cu, R = {}^tBu; \mathbf{4}{:}M = Cu, R = Ad \qquad (1)$$

The ^{77}Se NMR spectra of each cation in **1**−**4** exhibit only one resonance with chemical shifts of 1798, 1781, 1783, and 1773 ppm, respectively, compared to $\delta(^{77}Se)$ 1654 for $Se(N^tBu)_2$[6] and 1651 ppm for $Se(NAd)_2$.[14] The ^{14}N resonances were observed only for the ^{t}Bu derivatives **1** and **3** as broad singlets at 0 and −36 ppm, respectively. The ^{1}H NMR spectra of **1** and **3** show singlets at 1.62 and 1.77 ppm, respectively; those of the adamantyl analogues were not recorded.

Crystal Structures. The crystal structures of **1**·$2CH_2Cl_2$, **2**$(AdNH_3)(CF_3SO_3)$, **3**·2thf, and **4**·$1/2C_7H_8$ are shown together with the atomic numbering schemes in Figures 1−4, respectively. Selected bond parameters are summarized in Table 2.

The Se−N bond lengths in **1**−**4** span a range of 1.708(4)−1.729(6) Å, with the exception of the Se1−N1 bond distance of 1.749(7) Å in **2**. The slightly longer bond in **2** is probably a consequence of the presence of two adjacent bulky adamantyl groups. The Ag−N bonds in **1** show a rather wide range of 2.108(4)−2.226(4), while those in **2** span a narrow range of 2.152(7)−2.161(7) Å. The range of Cu−N bond lengths in **3** and **4** is

Table 3. Selected Bond lengths (Å) and angles (deg) from BPE/def-TZVP Optimized Geometries of $[M_2\{\mu\text{-}N,N'\text{-}Se(NR)_2\}_2]^{2+}$ (M = Cu, Ag; R = H, Me, ^{t}Bu, Ad)

	M···M	N−M	N−Se	N···N	N−M−N	M−N−Se	N−Se−N	N−M−N−Se	M−N−Se−N
$[Ag_2\{\mu\text{-}N,N'\text{-}Se(NH)_2\}_2]^{2+}$	2.924	2.127	1.729	2.710	174.2	131.3	103.2	0.0	0.0
$[Ag_2\{\mu\text{-}N,N'\text{-}Se(NMe)_2\}_2]^{2+}$	2.851	2.129	1.750	2.810	178.9	127.0	107.1	0.1	0.1
$[Ag_2\{\mu\text{-}N,N'\text{-}Se(N^tBu)_2\}_2]^{2+}$	2.816	2.138	1.750	2.800	178.6	126.5	106.1	13.8	7.6
$[Ag_2\{\mu\text{-}N,N'\text{-}Se(NAd)_2\}_2]^{2+}$	2.816	2.137	1.760	2.799	178.5	126.7	105.4	14.5	8.0
$[Cu_2\{\mu\text{-}N,N'\text{-}Se(NH)_2\}_2]^{2+}$	2.713	1.888	1.737	2.699	179.6	129.2	102.0	2.3	0.0
$[Cu_2\{\mu\text{-}N,N'\text{-}Se(NMe)_2\}_2]^{2+}$	2.612	1.892	1.755	2.784	175.9	124.1	105.0	165.9	7.8
$[Cu_2\{\mu\text{-}N,N'\text{-}Se(N^tBu)_2\}_2]^{2+}$	2.576	1.897	1.763	2.777	176.8	123.0	104.0	157.7	12.2
$[Cu_2\{\mu\text{-}N,N'\text{-}Se(NAd)_2\}_2]^{2+}$	2.551	1.895	1.778	2.785	178.0	121.4	103.1	150.8	15.7

Table 4. The RIMP2- and RICC2-Optimized M···M Distances (Å) of $[M_2\{\mu\text{-}N,N'\text{-}Se(NH)_2\}_2]^{2+}$ (M = Ag, Cu) Involving def2-TZVP, def2-TZVPP, and def2-QZVPP Basis Sets

$[Ag_2\{\mu\text{-}N,N'\text{-}Se(NH)_2\}_2]^{2+}$			$[Cu_2\{\mu\text{-}N,N'\text{-}Se(NH)_2\}_2]^{2+}$		
method	basis set	Ag···Ag (Å)	method	basis set	Cu···Cu (Å)
PBE	def2-TZVP	2.92	PBE	def2-TZVP	2.73
	def2-TZVPP	2.91		def2-TZVPP	2.73
	def2-QZVPP	2.89		def2-QZVPP	2.73
RIMP2	def2-TZVP	2.91	RIMP2	def2-TZVP	2.79
	def2-TZVPP	2.89		def2-TZVPP	2.77
	def2-QZVPP	2.84		def2-QZVPP	2.75
RICC2	def2-TZVP	2.85	RICC2	def2-TZVP	2.63
	def2-TZVPP	2.83		def2-TZVPP	2.60
	def2-QZVPP	2.78		def2-QZVPP	2.59

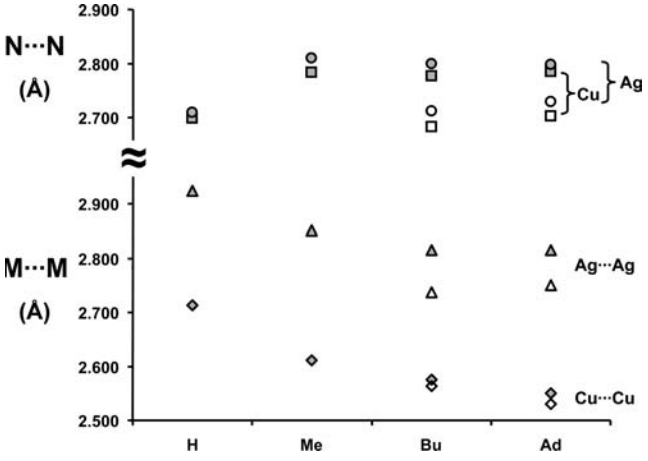

Figure 5. PBE/def-TZVP optimized M···M distances in the dications $[M_2\{\mu\text{-}N,N'\text{-}Se(NR)_2\}_2]^{2+}$ (M = Ag, Cu; R = H, Me, ^{t}Bu, Ad). Open circles, squares, triangles, and diamonds are experimental values.

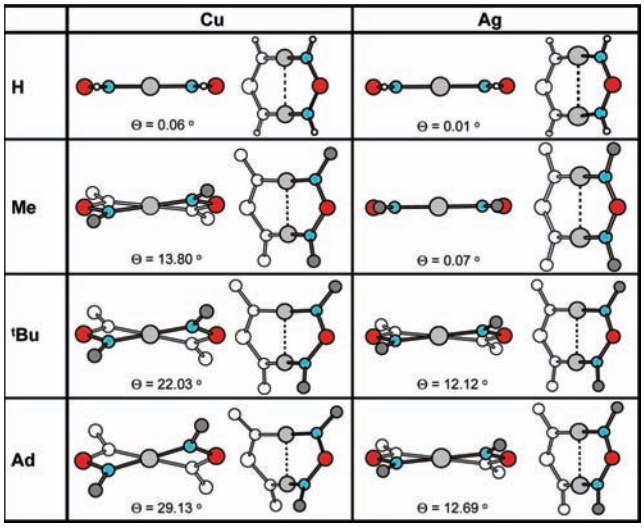

Figure 6. The PBE/def-TZVP optimized conformations of the metallacyclic framework in $[M_2\{\mu\text{-}N,N'\text{-}Se(NR)_2\}_2]^{2+}$ (M = Ag, Cu; R = H, Me, ^{t}Bu, Ad). The angle Θ indicates the deviation of $D_2M\cdots MD_2$ from planarity.

1.896(6)−1.917(4) Å. These values can be compared to those in related tellurium diimide complexes $[Ag_2\{\mu\text{-}N,N'\text{-}Te_2(N^tBu)_4\}_2](CF_3SO_3)_2$ [2.12(1)−2.144(9) Å] and $[Cu_2\{\mu\text{-}N,N'\text{-}Te_2(N^tBu)_4\}\{N\text{-}Te_2(N^tBu)_4\}_2](CF_3SO_3)_2$ [1.87(2)−1.90(2) Å].[9]

Each cation in **1**−**4** is a binuclear complex with two bridging selenium diimide ligands that coordinate through the nitrogen atoms and link the metal centers into a metallacycle. In the case of the silver cations in **1** and **2**, this geometrical arrangement of metal centers and ligands is reminiscent of that in **A** (Scheme 2),[9] except that the two N−Ag−N fragments in **1** and **2** are approximately coplanar, while those in **A** are almost perpendicular.[9] Such a metallacyclic arrangement of silver atoms has also been found in other complexes, for instance, in $[Ag_2(PPh_2CH_2SPh)_2](ClO_4)_2$,[12e] $[Ag_2(\mu\text{-}L)_2](CF_3SO_3)_2$ (L = 1-[(diphenylphosphino)methyl]-4-(2-pyridyl)piperazine),[25] and $[Ag_2(dptap)_2](NO_3)_2$ (dptap = 2-(2-pyridylimino)-2H-1,2,4-thia-diazolo [2,3-a] pyridine)[26] (see also ref 12 and discussion below). The N−Ag−N bond angles are 168.6(2)−176.6(2) and 157.7(3)° for **1** and **2**, respectively. The corresponding angles in $[Ag_2\{\mu\text{-}N,N'\text{-}Te_2(N^tBu)_4\}_2](CF_3SO_3)_2$ are 162.8(5)−163.8(5)°.[9]

Interestingly, the cations in the copper complexes **3** and **4** show a metallacyclic geometry similar to that of **1** and **2**,

(25) Kuang, S.-M.; Zhang, Z.-Z.; Wang, Q.-G.; Mak, T. C. W. *Inorg. Chem.* **1998**, *37*, 6090.
(26) Xu, X.-M.; Zhong, H.-M.; Zhang, H.-P.; Mo, Y.-R; Xie, Z.-X.; Long, L.-S.; Zheng, L.-S.; Mao, B.-W. *Chem. Phys. Lett.* **2004**, *386*, 254.

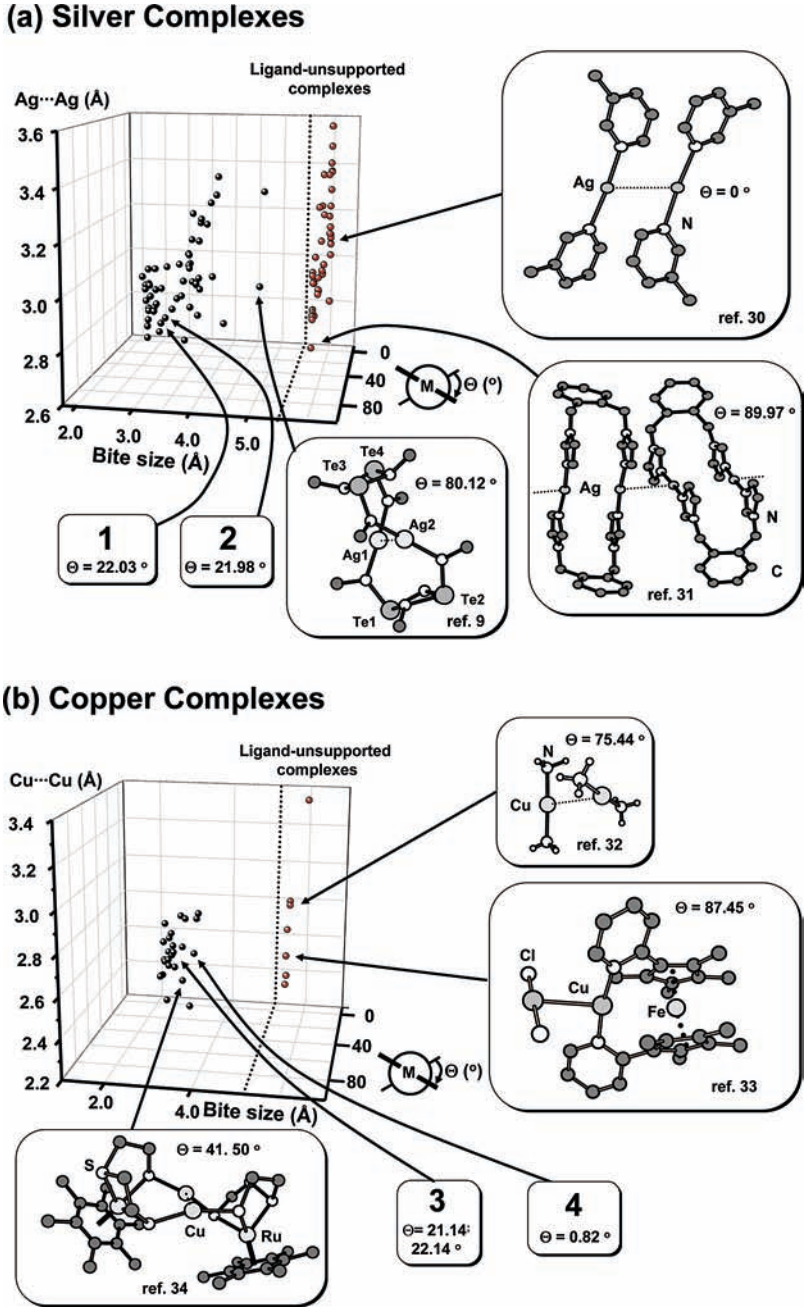

Figure 7. The survey of the dependence of (a) the Ag···Ag and (b) Cu···Cu distances (Å) on the bite size (D···D) (Å) and the deviation of the $D_2M\cdots MD_2$ fragment from planarity (angle Θ). The examples shown in the figure are redrawn from the crystallographic information given in refs 9 and 30−34.

even though the related tellurium diimide complex $[Cu_2\{\mu\text{-}N,N'\text{-}Te_2(N^tBu)_4\}\{N\text{-}Te_2(N^tBu)_4\}_2](CF_3SO_3)_2$ exhibits an open-chain dinuclear structure in which one tellurium diimide dimer acts as a bridging ligand between the metal centers.[9] The metallacyclic arrangement in **3** and **4** shows a slightly bent ring with the hinge along the Cu···Cu contact (see Figures 3 and 4). The N−Cu−N bond angles in **3** and **4** are in the range 157.9(2)−158.8(3)° and 160.2(2)−161.4(2)°, respectively.

Metallophilic Interactions. All four cations exhibit a M···M contact that is significantly shorter than the sum of van der Waals' radii of the coinage metals (see Table 2). They represent further examples of closed-shell d^{10}−d^{10} metallophilic interaction in the cases of Ag(I) and Cu(I).[11]

The early empirical[12a] and semiempirical[12b] studies inferred no net interaction and attributed the close M···M contacts to be dependent on the bite size of the bridging ligand.[27] With improvements in the level of theory, the presence of an attractive interaction was deduced. It has been attributed to dispersion forces[12c] and correlation,[12e,12h] relativistic, and excitation effects.[12h]

The PBE/def-TZVP optimized geometries of the $[M_2\{\mu\text{-}N,N'\text{-}Se(NR)_2\}_2]^{2+}$ (M = Cu, Ag; R = H, Me, ^{t}Bu, Ad) cations are presented in Table 3. It can be seen that the bond lengths and the bond angles are predicted rather well by this level of theory (cf. Table 2).

(27) For the purpose of this paper, bite size is defined as the distance between the donor atoms in the bidentate ligand.

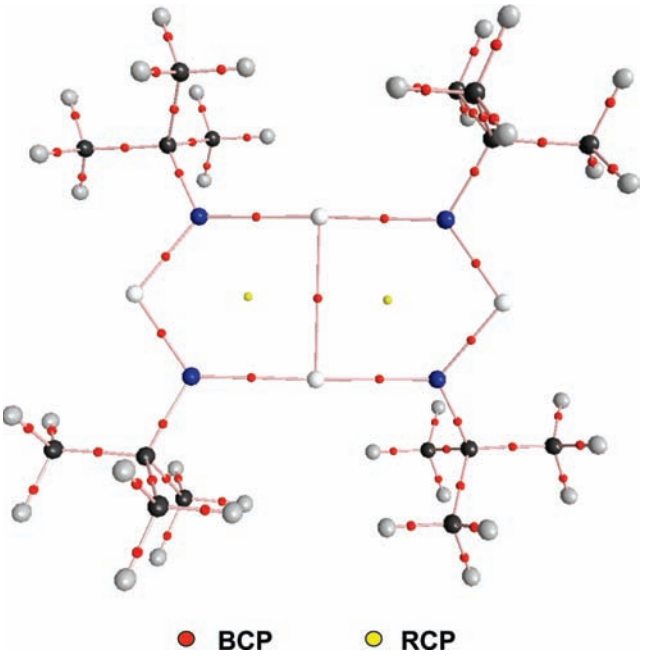

Figure 8. The bond and ring critical points for the optimized geometry of $[Ag_2\{\mu\text{-}N,N'\text{-}Se(N^tBu)_2\}_2]^{2+}$ calculated with the program AIM2000[21] using wave functions obtained by use of the program Gamess-US.[22a]

Even the computed M···M distances are in reasonable agreement with the experimental values, considering that the computations have been carried out on gas-phase species, whereas the experimental values have been determined in the solid state, and that DFT calculations are not suitable for modeling dispersion-type interactions. We therefore explored the geometries of $[M_2\{\mu\text{-}N,N'\text{-}Se(NH)_2\}_2]^{2+}$ (M = Cu, Ag) using a higher level of theory by optimizing their structures using RIMP2 and RICC2 computations and involving def2-TZVP, def2-TZVPP, and def2-QZVPP basis sets. While the general structural features were in agreement with the PBE/def-TZVP calculations, the M···M distances expectedly became shorter with higher-level calculations (see Table 4).

The trends in the M···M distances and bite sizes are shown in Figure 5. We note that both the optimized Ag···Ag and Cu···Cu distances become shorter, as the organic group R in $Se(NR)_2$ becomes bulkier. By contrast, with the exception of $[M_2\{\mu\text{-}N,N'\text{-}Se(NH)_2\}_2]^{2+}$, the bite size (N···N distance) remains virtually constant. Another trend is also apparent, as illustrated in Figure 6. With the increasing size of the organic substituent, the framework of the metallacyclic cation deviates from planarity. This puckering of the ring can be quantified by the angle Θ between the two D−M−D fragments (D represents the donor atom of the ligand):

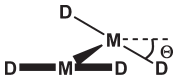

We explored the Cambridge Crystallographic Database[28] to gain more information about the factors influencing the Ag···Ag and Cu···Cu interactions. As seen from Figure 7, there may generally be a diffuse correlation between the M···M distance and the bite size, in particular, when the bite size is small. The variation, however, is rather large, and short M···M contacts are also found in both cases, even when the bite size is large (see Figure 7 for two illustrative examples). Furthermore, many ligand-unsupported complexes[29] also show M···M close contacts, although the M···M distances show a wide range for both silver and copper (see Figure 7). The experimental data indicate that the M···M distance correlates with the angle Θ between the two D−M−D fragments and is thus consistent with the PBE/def-TZVP results.

Table 5. Electron Density (ρ) and Delocalization Indices (DI) in the M···M Contact of $[M_2\{\mu\text{-}N,N'\text{-}Se(NR)_2\}_2]^{2+}$ Cations

	M = Cu		M = Ag	
	ρ (e Å^{-3})	DI	ρ (e Å^{-3})	DI
R = H	0.027	0.300	0.026	0.259
R = Me	0.032	0.339	0.030	0.289
R = ^{t}Bu	0.034	0.339	0.032	0.293
R = Ad	0.035	0.336	0.032	0.294

Two illustrative examples of ligand-unsupported complexes are shown for silver and copper complexes in Figure 7a and b, respectively. Tetrakis(β-picoline)disilver(I)bis(2-amino-5-chlorobenzenesulfonate) and *catena*-{tetrakis(μ-1,2-bis(1-imidazolylmethyl)benzene-*N*,*N*′)tetrasilver(I) tetrakis(hexafluoroantimonate)} display ligand-unsupported Ag···Ag distances of 3.123(1)[30] and 2.928(2) Å,[31] respectively. Analogous ligand-unsupported Cu···Cu distances for tetraamminedicopper(I)bis-{1,1-bis(4-hydroxyphenyl)-1-(4-oxyphenyl)-ethane} hydrate clathrate and *trans*-{1,1′-bis(2-pyridyl)octamethylferrocenyl-N,N′}dichlorodicopper(I) are 3.024(8)[32] and 2.810(2) Å,[33] respectively.

The orbital interactions in the M···M contact have been discussed on several occasions using different levels of theory.[12] In this contribution, we explored the bonding in all $[M_2\{\mu\text{-}N,N'\text{-}Se(NR)_2\}_2]^{2+}$ cations in **1**−**4** by utilizing atoms in molecules. All cations showed the presence of a bond critical point in the center of the line connecting the two metal atoms, as exemplified for $[Ag_2\{\mu\text{-}N,N'\text{-}Se(N^tBu)_2\}_2]^{2+}$ in Figure 8. Two ring critical points could also be observed. The electron density at the bond critical points and the delocalization indices are summarized in Table 5. The MP2 and CC2 computations show comparable results. These findings are consistent with recent computational studies carried out for related systems[12c,12e,12f] and indicate that there is a significant

(28) *ConQuest*; version 1.11; Cambridge Crystallographic Data Center: Cambridge, U. K., **2009**.

(29) In this context, the term "ligand-unsupported complexes" refers to complexes that do not contain bridging ligands between the two metal centers in question.

(30) Wu, H.; Dong, X.-W.; Ma, J.-F. *Acta Crystallogr.* **2006**, *62E*, m1227.
(31) Tan, H.-Y.; Zhang, H.-X.; Ou, H.-D.; Kang, B.-S. *Inorg. Chim. Acta* **2004**, *357*, 869.
(32) Zheng, S.-L.; Messerschmidt, M.; Coppens, P. *Angew. Chem., Int. Ed. Engl.* **2005**, *44*, 4614.
(33) Neumann, B.; Siemeling, U.; Stammler, H.-G.; Vorfeld, U.; Delis, J. G. P.; van Leeuwen, P. W. N. M.; Vrieze, K.; Fraanje, J.; Goubitz, K.; Zanello, P. *J. Chem. Soc., Dalton Trans.* **1997**, 4705.
(34) Shin, R. Y. C.; Tan, G. K.; Koh, L. L.; Vittal, J J.; Goh, L. Y.; Webster, R. D. *Organometallics* **2005**, *24*, 539.

interaction between the two metal atoms of the metallacyclic dications in **1**−**4**.

Conclusions

The first coinage metal complexes of selenium diimides have been prepared as triflate salts and structurally characterized. The dications $[M_2\{\mu\text{-}N,N'\text{-}Se(NR)_2\}_2]^{2+}$ (M = Ag, Cu; R = ^{t}Bu, Ad) in these salts form binuclear eight-membered MNSeNMNSeN rings that exhibit a short M···M contact indicative of a d^{10}−d^{10} closed-shell interaction. DFT calculations of the series of complexes $[M_2\{\mu\text{-}N,N'\text{-}Se(NR)_2\}_2]^{2+}$ (M = Ag, Cu; R = H, Me, ^{t}Bu, Ad) predict that the Ag···Ag and Cu···Cu distances become shorter as the organic group becomes bulkier. Concurrently, the metallacyclic framework deviates more significantly from planarity. A survey of related dinuclear Ag(I) and Cu(I) complexes indicates that, while the bite size of the bidentate ligand bridging the two metal centers may correlate with the M···M distance, especially when the bite size is short, the deviation of the $D_2M\cdots MD_2$ fragment (D is the donor atom of the bidentate ligand) from planarity has a more significant effect on the M···M distance. Atoms in molecules calculations for $[M_2\{\mu\text{-}N,N'\text{-}Se(NR)_2\}_2]^{2+}$ show the presence of a bond critical point between the metal atoms as well as two ring critical points in the centers of the two pseudo-five-membered MMNSeN rings.

Acknowledgment. Financial support from the Academy of Finland and NSERC (Canada), as well as a graduate school fellowship from the Ministry of Education in Finland (T.T.T.) and a scholarship from the Finnish Cultural foundation (M.R.), are gratefully acknowledged. We also thank the Finnish Centre of Scientific Computing for allocation of computational resources.

Supporting Information Available: Crystallographic information for **1**·$2CH_2Cl_2$, **2**$(AdNH_3)(CF_3SO_3)$, **3**·2thf, and **4**·$1/2C_7H_8$ (in CIF format). This material is available free of charge via the Internet at http://pubs.acs.org.